Ppb-level formaldehyde detection using a CW room-temperature interband cascade laser and a miniature dense pattern multipass gas cell

Lei Dong,[1,2,*] Yajun Yu,[1] Chunguang Li,[1] Stephen So,[3] and Frank K. Tittel[1]

[1]*Department of Electrical and Computer Engineering, Rice University, 6100 Main Street, Houston, TX 77005, USA*
[2]*State Key Laboratory of Quantum Optics and Quantum Optics Devices, Institute of Laser Spectroscopy, Shanxi University, Taiyuan 030006, China*
[3]*Sentinel Photonics, 11 Deer Park Dr, STE 208, Monmouth Junction, NJ 08852, USA*
**Lei.Dong@rice.edu*

Abstract: A ppb-level formaldehyde (H_2CO) sensor was developed using a thermoelectrically cooled (TEC), continuous-wave (CW) room temperature interband cascade laser (ICL) emitting at 3.59 μm and a miniature dense pattern multipass gas cell with >50 m optical path length. Performance of the sensor was investigated with two measurement schemes: direct absorption (DAS) and wavelength modulation spectroscopy (WMS). With an integration time of less than 1.5 second, a detection limit of ~3 ppbv for H_2CO measurement with precision of 1.25 ppbv for DAS and 0.58 ppbv for WMS, respectively, was achieved without zero air based background subtraction. An Allan-Werle variance analysis indicated that the precisions can be further improved to 0.26 ppbv @ 300s for DAS and 69 pptv @ 90 s for WMS, respectively. A side-by-side comparison between two measurement schemes is also discussed in detail.

OCIS codes: (280.3420) Laser sensors; (300.6340) Spectroscopy, infrared; (140.5965) Semiconductor lasers, quantum cascade.

References and links

1. *OSHA Standards* – 29 CFR 1910.1048 (2006).
2. R. E. Crossgrove, *Spacecraft Maximum Allowable Concentrations for Selected Airborne Contaminants,* Vol.1–4 (National Academy of Sciences, 1994–2000).
3. B. P. Wert, M. Trainer, A. Fried, T. B. Ryerson, B. Henry, W. Potter, W. M. Angevine, E. Atlas, S. G. Donnelly, F. C. Fehsenfeld, G. J. Frost, P. D. Goldan, A. Hansel, J. S. Holloway, G. Hubler, W. C. Kuster, D. K. Nicks, Jr., J. A. Neuman, D. D. Parrish, S. Schauffler, J. Stutz, D. T. Sueper, C. Wiedinmyer, and A. Wisthaler, "Signatures of terminal alkene oxidation in airborne formaldehyde measurements during TexAQS 2000," J. Geophys. Res. **108**(D3), 4104 (2003).
4. J. Chen, S. So, H. Lee, M. P. Fraser, R. F. Curl, T. Harman, and F. K. Tittel, "Atmospheric formaldehyde monitoring in the Greater Houston area in 2002," Appl. Spectrosc. **58**(2), 243–247 (2004).
5. H. I. Schiff, D. R. Hastie, G. I. Mackay, T. Iguchi, and B. A. Ridley, "Tunable diode laser systems for measuring trace gases intropospheric air," Environ. Sci. Technol. **17**(8), 352A–364A (1983).
6. H. Dahnke, G. von Basum, K. Kleinermanns, P. Hering, and M. Mürtz, "Rapid formaldehyde monitoring in ambient air by means of mid-infrared cavity leak-out spectroscopy," Appl. Phys. B **75**(2-3), 311–316 (2002).
7. D. Rehle, D. Leleux, M. Erdelyi, F. Tittel, M. Fraser, and S. Friedfeld, "Ambient formaldehyde detection with a laser spectrometer based on difference-frequency generation in PPLN," Appl. Phys. B **72**(8), 947–952 (2001).
8. D. G. Lancaster, A. Fried, B. Wert, B. Henry, and F. K. Tittel, "Difference-frequency-based tunable absorption spectrometer for detection of atmospheric formaldehyde," Appl. Opt. **39**(24), 4436–4443 (2000).
9. P. Maddaloni, P. Malara, G. Gagliardi, and P. De Natale, "Two-tone frequency modulation spectroscopy for ambient-air trace gas detection using a portable difference-frequency source around 3 μm," Appl. Phys. B **85**(2-3), 219–222 (2006).
10. M. Angelmahr, A. Miklos, and P. Hess, "Photoacoustic spectroscopy of formaldehyde with tunable laser radiation at the parts per billion level," Appl. Phys. B **85**(2-3), 285–288 (2006).
11. J. Li, U. Parchatka, and H. Fischer, "A formaldehyde trace gas sensor based on a thermoelectrically cooled CW-DFB quantum cascade laser," Anal. Methods **6**(15), 5483–5488 (2014).

#242289 Received 3 Jun 2015; revised 10 Jul 2015; accepted 16 Jul 2015; published 22 Jul 2015

12. J. H. Miller, Y. A. Bakhirkin, T. Ajtai, F. K. Tittel, C. J. Hill, and R. Q. Yang, "Detection of formaldehyde using off-axis integrated cavity output spectroscopy with an interband cascade laser," Appl. Phys. B **85**(2-3), 391–396 (2006).
13. G. Wysocki, Y. Bakhirkin, S. So, F. K. Tittel, C. J. Hill, R. Q. Yang, and M. P. Fraser, "Dual interband cascade laser based trace-gas sensor for environmental monitoring," Appl. Opt. **46**(33), 8202–8210 (2007).
14. F. Capasso, "High-performance midinfrared quantum cascade lasers," Opt. Eng. **49**(11), 111102 (2010).
15. I. Vurgaftman, C. L. Canedy, C. S. Kim, M. Kim, W. W. Bewley, J. R. Lindle, J. Abell, and J. R. Meyer, "Mid-infrared interband cascade lasers operating at ambient temperatures," New J. Phys. **11**(12), 125015 (2009).
16. I. Vurgaftman, W. W. Bewley, C. L. Canedy, C. S. Kim, M. Kim, C. D. Merritt, J. Abell, J. R. Lindle, and J. R. Meyer, "Rebalancing of internally generated carriers for mid-infrared interband cascade lasers with very low power consumption," Nat. Commun. **2**, 585 (2011).
17. S. Lundqvist, P. Kluczynski, R. Weih, M. von Edlinger, L. Nähle, M. Fischer, A. Bauer, S. Höfling, and J. Koeth, "Sensing of formaldehyde using a distributed feedback interband cascade laser emitting around 3493 nm," Appl. Opt. **51**(25), 6009–6013 (2012).
18. G. Overton, "METROLOGY: New multipass gas cells beat conventional designs," Laser Focus World, August issue (2013).
19. K. Krzempek, M. Jahjah, R. Lewicki, P. Stefański, S. So, D. Thomazy, and F. K. Tittel, "CW DFB RT diode laser-based sensor for trace-gas detection of ethane using a novel compact multipass gas absorption cell," Appl. Phys. B **112**(4), 461–465 (2013).
20. P. Werle, R. Mücke, and F. Slemr, "The limits of signal averaging in atmospheric trace-gas monitoring by tunable diode-laser absorption spectroscopy (TDLAS)," Appl. Phys. B **57**, 131–139 (1993).
21. P. Werle, F. Slemr, M. Gehrtz, and C. Bräuchle, "Quantum-limited FM-spectroscopy with a lead-salt diode laser," Appl. Phys. B **49**, 99–108 (1989).
22. http://en.wikipedia.org/wiki/Accuracy_and_precision.
23. D. Richter, P. Weibring, J. G. Walega, A. Fried, S. M. Spuler, and M. S. Taubman, "Compact highly sensitive multi-species airborne mid-IR spectrometer," Appl. Phys. B **119**(1), 119–131 (2015).
24. C. Roller, A. Fried, J. Walega, P. Weibring, and F. Tittel, "Advances in hardware, system diagnostics software, and acquisition procedures for high performance airborne tunable diode laser measurements of formaldehyde," Appl. Phys. B **82**(2), 247–264 (2006).

1. Introduction

Formaldehyde (H_2CO) is widely used in the manufacture of industrial and consumer products, especially in building materials and numerous household products, such as wood-based panels. Formaldehyde escaping from these materials may lead to poor indoor air levels that adversely affect human health. The permissible H_2CO exposure limit (PEL) is 750 ppbv averaged for an eight-hour work day and a short term exposure limit (STEL) of 2 ppmv averaged over 15 min, which has been established by the US Occupational Safety and Health Administration [1]. For the spacecraft, NASA has more conservative maximum allowable concentrations, in which case the upper limits range from 400 ppbv for short term (1h) exposure down to 40 ppbv for seven to 180 day lasting space missions [2]. Furthermore, formaldehyde is a key intermediate in photooxidation processes of many hydrocarbons. H_2CO plays an important role in understanding of tropospheric ozone formation chemistry [3]. Formaldehyde concentration levels in urban environment range typically from ~2 to 45 ppbv, which is primarily from fugitive industrial emissions and motor vehicles, and secondarily from the photochemical oxidation of volatile organic compounds (VOCs) due to intense sunlight [4]. Hence, a ppb-level formaldehyde detection with a fast time response is desired for both indoor or outdoor environmental monitoring.

Real-time, quantitative concentration measurements of formaldehyde based on laser spectroscopy have been demonstrated using different laser sources, including lead salt lasers [5], CO-overtone sideband lasers [6], difference-frequency generation (DFG) [4,7–9], optical parametric oscillators (OPO) [10], quantum cascade lasers (QCLs) [11] and interband cascade lasers (ICLs) [12,13]. Lead salt lasers require cryogenic cooling (typically below 130 K), which is not practical for field measurements activities. CO-overtone sideband lasers, DFG and OPO sources have a large footprint and weight which limit their applications where small size and low weight are important. Commercially available QCLs offer the advantages of a high power (~10-100 mW), small size and light weight covering the spectral range from > 4 μm and < 12 μm [14]. In the case of H_2CO, the strongest absorption band is located at 3.6 μm. Commercial ICLs tend to emit at wavelengths between 3 and 4 μm. But the early versions require cryogenic

#242289 Received 3 Jun 2015; revised 10 Jul 2015; accepted 16 Jul 2015; published 22 Jul 2015

cooling [12,13]. The new generation of ICLs is a promising alternative [15], offering the advantages of room temperature operation, lower threshold drive current requirements and hence lower power consumption than QCLs [16]. For example, S. Lundqvist et. al. [17], in 2012, employed a distributed feedback (DFB) ICL emitting around 3493 nm with the operation temperature of −8.5°C to detect H_2CO, obtaining a resolution limit better than 1ppm × m. In this manuscript, a H_2CO sensor was developed using a compact continuous-wavelength (CW) room-temperature ICL emitting at 3359 nm with a novel miniature dense pattern multipass gas cell (MGC) [18,19]. The ultra-compact MGC has a 54.6 m optical path length in a physical size of 17 × 6.5 × 5.5 cm^3, which is more than ten times smaller than conventional and commercial designs with equivalent sensitivity. Two measurement schemes, direct absorption spectroscopy (DAS) and 2*f* wavelength-modulation spectroscopy (2*f*-WMS), were compared and assessed by means of ICL based H_2CO sensor with the MGC, which resulted in a sensor capable of detecting ppb levels of H_2CO concentrations.

2. Line selection and ICL characterization

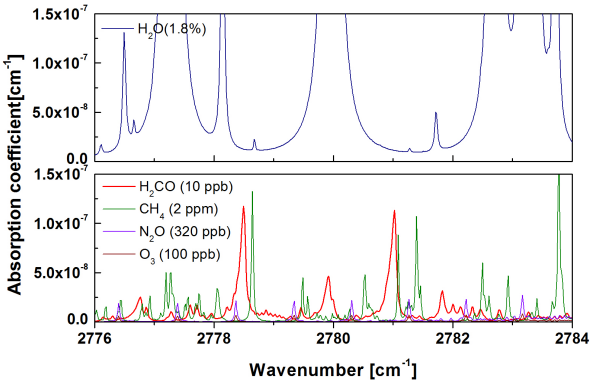

Fig. 1. HITRAN simulation of the H_2CO absorption spectrum within the ICL tuning range and potential interference from other atmospheric species (CH_4, N_2O and O_3). The total pressure is 200 Torr at 296 K temperature.

H_2CO has strong ν_1, ν_2 and ν_5 fundamental vibration bands centered at 2785, 1750 and 2850 cm^{-1}, respectively. We selected the ν_1 vibration band centered at 2785 cm^{-1} since its absorption coefficient is the largest. The potential spectral interferences caused by other atmospheric species are mainly from methane (CH_4), nitrous oxide (N_2O), ozone (O_3) and water (H_2O). Two interference-free H_2CO absorption lines centered at 2778.5 cm^{-1} and 2781.0 cm^{-1}, respectively, were identified to be optimal for H_2CO detection. A spectral simulation for typical experimental conditions using the HITRAN database was plotted in the bottom part of Fig. 1 with 10 ppb H_2CO, 2 ppm CH_4, 320 ppb N_2O and 100 ppb O_3. The 1.8% water spectra were separately plotted in the top part of Fig. 1 in order to identify clearly interfering H_2O absorption lines. These used concentration values of the gas components are typical ambient concentration levels. The 2871.0 cm^{-1} absorption line was used in the development of our H_2CO sensor system based on our HITRAN analysis.

A CW DFB ICL was mounted in a TO66 header from nanoplus Nanosystems and Technologies GmbH (http://www.nanoplus.com/) emitting single-mode radiation at a center wavelength of 3599 nm, in order to target the two selected H_2CO absorption lines. The TO66 header was enclosed in a 5 × 5 × 5 cm^3 cubic heat sink with a thermal electrically cooler (TEC). The ICL was operated typically in a temperature range between 30°C and 40°C. A Fourier transform infrared (FTIR) spectrometer (Thermo Scientific, model Nicolet 8700) and a power meter (Ophir Optronics, model 3A) were employed to measure the output wavelength and power of the ICL, respectively, at different ICL currents. The measured L-I-V

#242289 Received 3 Jun 2015; revised 10 Jul 2015; accepted 16 Jul 2015; published 22 Jul 2015

(light-current-voltage) curve at an operational ICL temperature of 35°C is shown in Fig. 2(a). The output power is ~3.8 mW, when the ICL was operated at a typical operating current of 52 mA and temperature of 35°C. The ICL can be tunable between 2776.5cm^{-1} and 2783.5 cm^{-1}, as shown in Fig. 2(b). This spectral range covers the two identified target lines marked with red lines in Fig. 2(b). Based on the Fig. 2(b), the current and temperature tuning coefficients of the ICL are –0.138 cm^{-1}/mA and –0.177 cm^{-1}/°C.

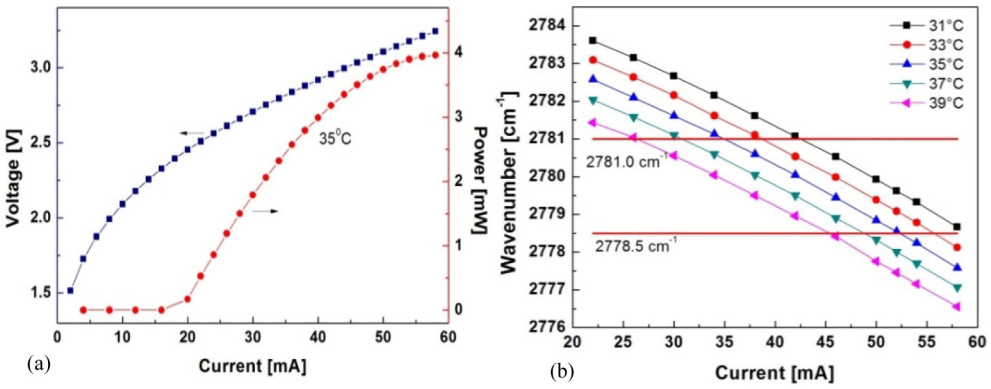

Fig. 2. (a) L-I-V curve of the 3.599 μm CW, DFB ICL; (b) DFB ICL current tuning at different DFB ICL operating temperatures.

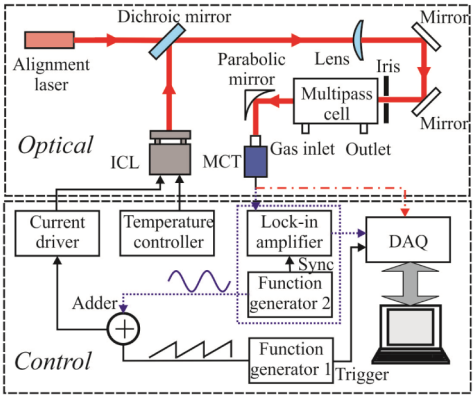

Fig. 3. Schematic of H_2CO gas sensor system based on a novel compact multipass gas cell using a 3.599 μm CW, DFB, ICL excitation source.

3. H_2CO gas sensor configuration

The H_2CO sensor architecture is depicted in Fig. 3. In the optical part, a semiconductor laser diode (alignment laser), emitting visible radiation at 630 nm, was employed as a guide beam of the invisible mid-infrared (mid-IR) beam in order to simplify the optical alignment process. The two laser beams, visible and mid-IR, were combined by means of a dichroic mirror (ISO optics, model BSP-DI-25-3). Then the combined laser beam was coupled into the MGC with a 54.6 m optical path length (developed by Sentinel Photonics) by using a mode matching lens of 200 mm focal length. The enclosure of the MGC was made of super invar with a typical mean coefficient of thermal expansion of 10^{-6}/°C. In addition, the enclosure of the MGC has a gas inlet and outlet. The mode matching lens had its focusing point at the entry of the MPC. An adjustable iris was also placed at the MPC entry in order to filter out high order spatial beam modes. After 435 beam passes, the collimated ICL beam exiting the MPC was focused onto a

#242289 Received 3 Jun 2015; revised 10 Jul 2015; accepted 16 Jul 2015; published 22 Jul 2015

TEC, mercury-cadmium-telluride (MCT) detector (Vigo, PVI-4TE-4) using a 35 mm focal length parabolic mirror.

The temperature and current of the ICL were operated using a commercial temperature controller (Thorlabs, model TED 200 C) and a current driver (ILX, model LDX-3220), respectively. The control parts for the two measurement schemes (DAS and WMS) were different. When using the DAS scheme, the instruments, including a lock-in amplifier and a function generator in purple dotted block of Fig. 3, were disabled. Only function generator 1 (Stanford model DS345, http://www.thinksrs.com/products/DS345.htm) supplied a saw tooth wave to the current driver to scan the ICL wavelength over the target line. An acquisition system including a DAQ card and a laptop was triggered by function generator 1 to acquire the spectra from the MCT (red dash-dot line). On the other hand, when using the WMS scheme, the lock-in amplifier (Stanford, model SR830) and Function generator 2 (a part of SR830), were activated. Function generator 2 generated a small amplitude sinusoidal wave. After combining the saw tooth wave via an electrical adder, it was introduced to the current driver to dither the ICL wavelength. The lock-in amplifier was set in the 2*f* mode to demodulate the signal from the MCT using the sync signal from function generator 2. The acquisition system acquires the second harmonic spectra from the lock-in amplifier (purple dot line instead of red dash-dot line). In order to eliminate the disturbance from the environmental temperature variations, the MGC was wrapped by a layer of thermal insulation material and its temperature was controlled at 26°C using a thermistor, a heater strip and temperature PID controller (Omega, model CNi3222). A pressure controller and a vacuum pump were placed upstream and downstream to the MGC, controlling and maintaining the system pressure, respectively. A constant flow rate of 200 SCCM was used here.

4. Sensor performance with DAS

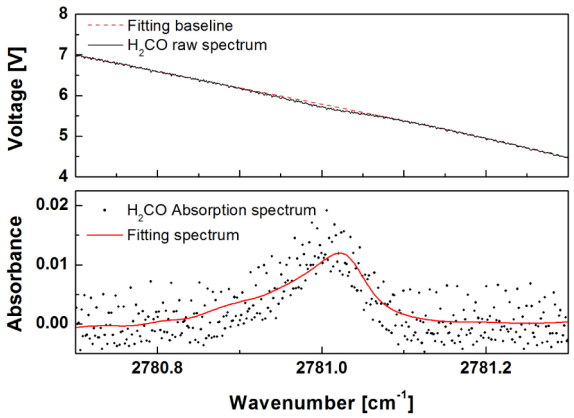

Fig. 4. Typical example of fitting strategy for a direct absorption spectrum of H_2CO at a 208 ppbv concentration level.

When using the DAS sensor configuration, the ICL temperature and current were set to 35°C and 36.2 mA, which correspond to a wavelength of ~2781 cm^{-1}. The pressure in the MGC was set to 200 Torr in order to avoid spectral interference from other atmospheric species. The operating pressure is a compromise between sensor detection sensitivity and selectivity. In fact the detection sensitivity did not decrease significantly below the value at atmospheric pressure when the pressure was reduced to 200 Torr. This is due to the fact that in pressure broadening, the spectral amplitude is insensitive to the pressure until Doppler broadening dominates. Function generator 1 generated a 500Hz saw tooth wave with a peak-to-peak amplitude of 280 mV, resulting in ICL wavelength tuning between 2780.5cm^{-1} to 2781.3cm^{-1}. The sampling rate of the DAQ card was set to 250 kHz. As a result, each H_2CO spectra include 500 data points.

#242289 Received 3 Jun 2015; revised 10 Jul 2015; accepted 16 Jul 2015; published 22 Jul 2015

After the DAQ card was triggered by the Function generator 1, it acquired data for 344 ms to avert time delays caused by frequent triggering. Thus 86 k data points were collected, which corresponds to 172 H_2CO spectra. The spectrum in the top part of Fig. 4 (solid line) is the result of averaging 172 spectra. The electronic system bandwidth was 300 kHz determined by the preamplifier of the MCT detector. Spectral averaging resulted in an effective bandwidth of 1.74 kHz.

After spectral averaging, the first 50 data points were deleted due to the fact that they correspond to the steep falling edge of the saw tooth wave. In order to remove the effect of the power variations caused by current changes, the two wings of the spectrum were extracted and a polynomial fitting was applied to obtain the H_2CO spectral base line I_0, as shown in the top part of Fig. 4 (dash line). Subsequently the absorption spectrum was calculated via Beer-Lambert law $-\ln(I/I_0)$ where the intensity I is given by the data points, and its abscissa was converted from data points to wavenumber by means of a quadratic polynomial. As the temperature and pressure in the MGC are constant, the theoretical spectrum, which was used to fit the experimental spectrum, did not have to be calculated every time. Instead, a calculated 500 ppbv H_2CO spectrum at a pressure of 200 Torr and temperature of 26 °C was prepared in advance and stored in the associated laptop memory. The Levenberg-Marquardt nonlinear least-squares fitting algorithm was employed, as shown in the bottom part of Fig. 4, to return a scaling factor from the calculated to the experimental spectrum. The product of the 500 ppbv and the scaling factor provides the H_2CO measurement result. The data processing routine was prepared using Labview (http://www.ni.com/labview/). Data processing required 156ms, and thus the result output rate of the H_2CO sensor is 2 Hz with a 69% duty cycle (data acquisition time of a 344ms/measurement time 500ms) [20].

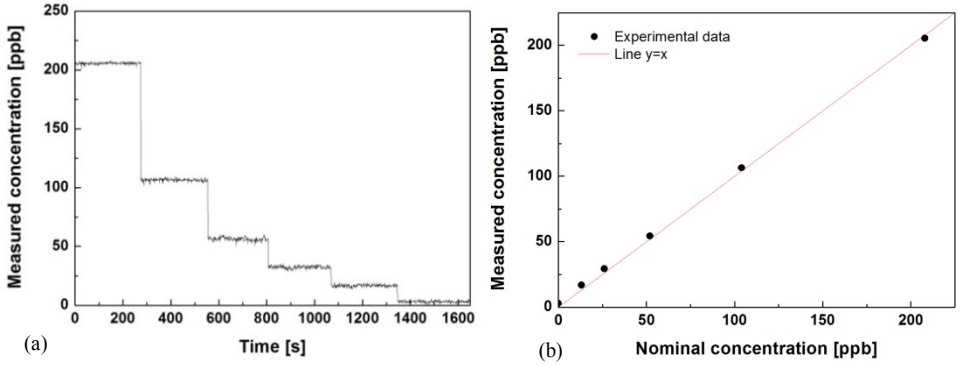

Fig. 5. (a) H_2CO concentration response of sensor operating in DAS; (b) Linear dependence of the measured concentration as a function of the H_2CO nominal concentrations.

A permeation tube based trace gas generator (Kin-Tek Laboratories, Inc., model 491M) was used for the performance assessment and linearity testing of the DAS sensor. The generated H_2CO concentration in the carrier gas was determined by the gas mass flow rate passing through the sensor system, when reaching a maximum stable value of 268 ppbv at the minimum flow of 100 sccm. Figure 5(a) shows the time series of the concentration measurements at five different flow rates, which correspond to nominal concentrations, 208 ppbv, 104 ppbv, 52 ppbv, 26 ppbv and 13 ppbv. Finally, pure nitrogen was introduced. The linearity of the DAS based sensor was evaluated. The measured concentrations for each step were averaged and plotted against the nominal concentrations as shown in Fig. 5(b). A line of y = x was also plotted. The behavior of the measured concentrations following the line y = x verified an excellent linear response of the DAS based H_2CO sensor system.

#242289 Received 3 Jun 2015; revised 10 Jul 2015; accepted 16 Jul 2015; published 22 Jul 2015

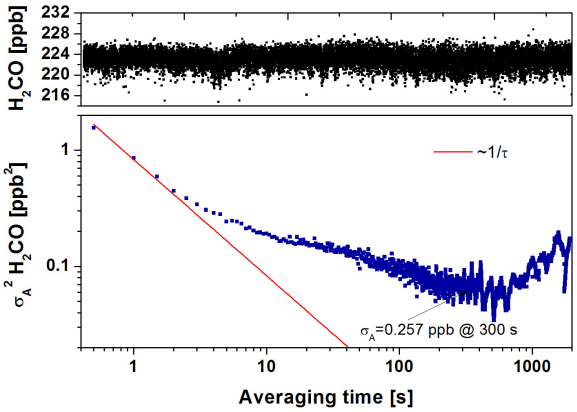

Fig. 6. Allan variance calculated from a direct absorption spectrum measurements of H_2CO for a concentration of 224 ppbv with a 0.5 s sampling rate.

Additional measurements of a H_2CO sample with 224 ppbv over time periods of ~2.6 hours were performed. An Allen-Werle variance is utilized to analyze the stability and precision of the H_2CO sensor system. As shown in Fig. 6, the Allan variance σ_A^2 is plotted on a log-log scale versus averaging time. The plot indicates that measurement precision, σ_A, is 1.25 ppbv with a 0.5 s measurement time. The Allan plot shows an optimum integration time of ~300 s, corresponding to a precision of ~0.257 ppbv. The decreasing red solid line indicates the theoretically expected behavior (proportional to $1/\tau$) of a system with the white noise dominated region prior to when system drifts start to dominate.

5. Sensor performance with 2*f*-WMS

With 2*f*-WMS sensor configuration, the temperature and current of the laser source, and the pressure in the MGC, remain unchanged. To produce 2*f*-WMS signals, the frequency of the saw tooth wave from function generator 1, was reduced from 500 Hz to 5Hz, due to the bandwidth limit of the lock-in amplifier. A sinusoidal modulation of 43 kHz with a peak-to peak amplitude of 200 mV from function generator 2 was, after combined with the saw tooth wave, supplied to the ICL. Such modulation amplitude corresponds to an optimal modulation depth to obtain the maximum 2*f* signal amplitude with 200 Torr. The 2nd harmonic signal was demodulated using the lock-in amplifier with a time constant of 3 ms and a filter slope of 12 dB, resulting in an equivalent noise bandwidth (ENBW) of Δf = 41.7Hz. With such integration parameters the observed spectral lines were not distorted by lock-in detection. The sampling rate of the DAQ card was set in 2.5 kHz. After triggered by Function generator 1, it implemented a continuous acquisition for 3500 data points, which took 1.4 s and resulted in an effective bandwidth of 6.0 Hz. The 3500 data points include 7 H_2CO 2*f* spectra. As the same for DAS data processing, the first 50 data points were deleted after the 7 spectra were averaged. A 260 ppbv H_2CO 2*f* spectrum acquired from the experiment was stored in the memory of the laptop. As previously the Levenberg-Marquardt nonlinear least-squares fitting algorithm was employed to obtain the scaling factor and calculate the measured H_2CO concentration. Figure 7 shows an example of the spectrum fitting for an 11 ppbv H_2CO sample. The data processing time was reduced to 100ms due to no need of fitting baseline and linearizing the spectrum. Hence the resulting output rate of the H_2CO sensor is 0.67 Hz, i.e. 1.5s/point with a 93% duty cycle.

#242289 Received 3 Jun 2015; revised 10 Jul 2015; accepted 16 Jul 2015; published 22 Jul 2015

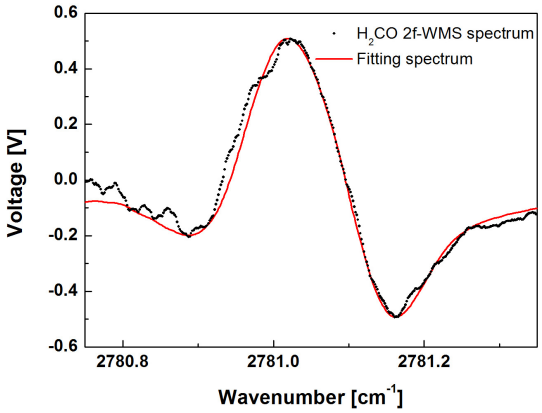

Fig. 7. An example of fitting strategy for H_2CO 2*f* wavelength modulation spectrum for a concentration of 11 ppbv.

The linearity of the 2*f*-WMS based H_2CO sensor was evaluated by measuring its response to the different H_2CO concentrations. Three different flow rates of the trace gas generator, which correspond to nominal concentrations of 45 ppbv, 23 ppbv and 11 ppbv were applied to the 2*f*-WMS based H_2CO sensor. As previously, pure nitrogen was introduced to check the zero background level. The results are plotted in Fig. 8(a). Data for each step are averaged and plotted against the H_2CO concentrations in Fig. 8(b). The relationship of y = x between the measured and nominal concentrations confirm the linearity of the sensor response to H_2CO concentrations.

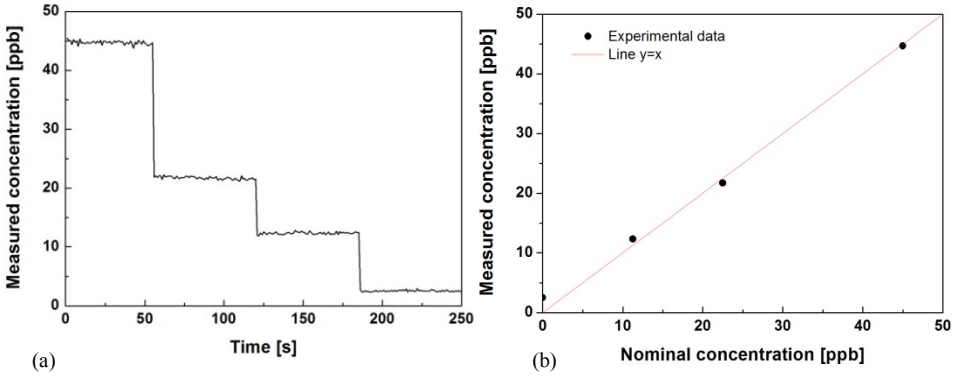

Fig. 8. (a) H_2CO concentration response of the sensor with 2*f*-WMS; (b) Linear dependence of the measured concentration as a function of the H_2CO nominal concentration.

The performance of the 2*f*-WMS system, characterized by the Allen-Werle variance, has been investigated and the results are shown in Fig. 9. The Allen-Werle variance was generated from a 35 min continuous measurement for a 29 ppb H_2CO sample. The result shows that measurement precision with the 1.5 s measurement time is $\sigma_A \approx 0.58$ ppbv. The Allan-Werle plot yields an optimum integration time of ~90 s with a precision of ~69 pptv.

#242289 Received 3 Jun 2015; revised 10 Jul 2015; accepted 16 Jul 2015; published 22 Jul 2015

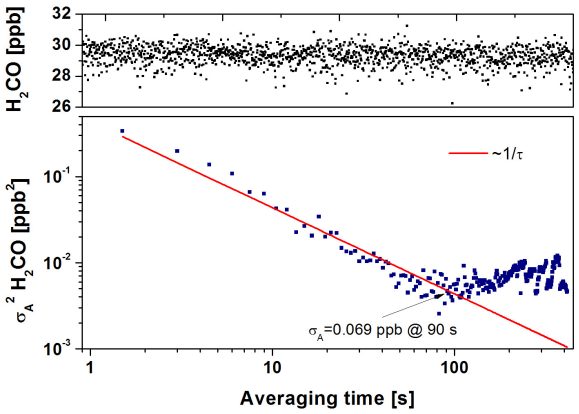

Fig. 9. Allan variance calculated from a 2f spectrum measurement of H_2CO with a concentration of 29 ppbv with a 1.5 s sampling rate.

6. Discussions

DAS is the simplest realization in laser absorption spectroscopic techniques for gas analysis. The most attractive advantage of DAS is its ability to offer absolute quantitative measurement of species without sensor calibration as the concentration of the target species can be calculated from the relative change of the intensity according to Lambert-Beer's law. The drawback is that the result depends on a measurement of a small change at a high power level. As a result, noise, mainly in low frequency region, introduced by the light source or the transmission through the optical system will deteriorate the detection sensitivity of this technique. On the other hand, the better technique is 2*f*-WMS, in which the spectral signal is shifted to high frequency region to avert the low frequency noise, often referred to as 1/*f* noise. This procedure can improve the measurement precision. If it is true that the measured DAS and 2*f*-WMS are only subject to random noise, further averaging of these measured spectra should then improve the measurement precision and detection limit according to a square-root relationship [21]. This can be observed from the Allan variance plots reported in Fig. 6 and Fig. 9 which indicate that a DAS measurement precision of 1.25 ppbv, obtained for 0.5s, was improved to 0.257 ppbv at 300s, while with 2*f*-WMS a higher measurement precision of 0.58 ppbv was achieved for 1.5 s and further lowered to 69 pptv at 90s. Moreover, the Allan variance for 2*f*-WMS follows the white noise before averaging time of 100 s, while there is a deviation between the white noise and the Allan variance for DAS, after 2s averaging time, which delays the optimum averaging time. However, an important thing to be kept in mind is that the 2*f*-WMS signal is affected by any power fluctuations and thus it has to be normalized to optical power in practical applications. There is no such problem for DAS.

The noise of the sensor system affecting detection limit may be categorized into two noise sources: electronic noises from lasers, detectors, and additional electronics, and interference noises due to spectral and optical interferences. The TE-cooled Vigo MCT detector has a detectivity of ~6×10^{11} cm•$Hz^{1/2}$/W with a noise level of ~5 nV•$Hz^{1/2}$ from its preamplifier. The ICL was also observed to produce photon noise when the laser beam was incident on the detector. From the H_2CO spectrum data, interference fringes due to unwanted etalons are the primary factor limiting signal-to-noise ratio (SNR), but not laser noise or detector noise. When pure nitrogen was introduced into the sensor system, it was observed that the fringes have a stable pattern and do not move even after increasing the number of spectra averaging. This implies that the signal averaging just can improve the measurement precision, but cannot improve the detection limit. The magnitude of the unwanted interference fringe corresponds to an equivalent absorbance between 10^{-3} and 10^{-2}, and is associated with the effect of optical scatter since the ultra-compact cell has a dense multi-pass pattern. The presence of optical

#242289 Received 3 Jun 2015; revised 10 Jul 2015; accepted 16 Jul 2015; published 22 Jul 2015

fringes affects the measurements accuracy [22] especially at low concentration levels, because the measured concentration levels have a slightly positive deviation from the nominal concentrations with the concentrations decreasing, as shown in Fig. 5(b) and Fig. 8(b). In principle, the problem of fringe limitation can be solved by subtraction of a zero spectrum from the measured spectrum, usually performed by measuring alternatively the spectrum of the ambient air and the spectrum of zero air [11, 23,24]. The current sensor system did not adopt the scheme, which simplifies the sensor configuration, gas sampling system and data processing, and increases the duty cycle for spectra acquisition. According to Fig. 5 and Fig. 8, DAS and 2*f*-WMS have a ~3 ppbv and ~2.5 ppbv detection limit, respectively, which are the results that the spectral fitting algorithm yields in the present of the optical fringe. The two realized detection limits indicate the potential use of the reported sensor technology for H_2CO environmental monitoring.

7. Conclusions

We have developed an ICL based sensor using MGC for ppb-level formaldehyde detection. A novel dense pattern MGC can provide a >50 m optical path length within a small sampling volume of 220 ml to facilitate a fast gas exchange. The CW room temperature ICL can access the strongest H_2CO absorption band. The combination of the two techniques has the potential ability to offer compact, high sensitive and low-power-cost trace gas sensors. Two different measurement schemes, DAS and 2*f*-WMS, were employed to assess the H_2CO sensor performance. In contrast to DAS, the 2*f*-WMS has the better measurement precision, which can achieve 69 pptv for a data acquisition time of 90s. However both measurement schemes have a detection limit of ~3 ppbv which is limited by the interference fringes due to unwanted etalons. In Ref [9], P. Maddaloni et al. have experimentally compared the performance of DAS and two-tone frequency modulation spectroscopy (TTFMS) techniques for ambient-air trace gas detection using a 13 m MGC and a DFG based excitation source at ~3 μm, which is in the same spectral range used in our work. With TTFMS, an enhancement of a factor of 100 in the SNR was achieved, which resulted in a H_2CO detection limit of 0.8 ppbv with 1 s averaging time. However, the DFG light source used in Ref [9] required a radio frequency source of ~400 MHz and two mixers to demodulate two-tone frequency modulation, which makes such a sensor system considerably larger than the reported ICL based sensor. The reported sensor system can be easily adapted to other trace gases by changing the ICL chip and detector.

Acknowledgments

Lei Dong acknowledges support by National Natural Science Foundation of China (Grant #s. 61275213, 61108030). Frank Tittel acknowledges support by the National Science Foundation (NSF) ERC MIRTHE award, the Robert Welch Foundation (Grant C-0586) and a NSF phase II SBIR (Grant No. IIP-1230427).

#242289 Received 3 Jun 2015; revised 10 Jul 2015; accepted 16 Jul 2015; published 22 Jul 2015